BIOCHEMISTRY
including biophysical chemistry & molecular biology

Accelerated Publication

pubs.acs.org/biochemistry

Three-Dimensional Structure and Determinants of Stability of the Iron−Sulfur Cluster Scaffold Protein IscU from *Escherichia coli*

Jin Hae Kim,[‡] Marco Tonelli,[§] Taewook Kim,[‡] and John L. Markley*[,‡,§]

[‡]Department of Biochemistry, [§]National Magnetic Resonance Facility at Madison, University of Wisconsin-Madison, 433 Babcock Drive, Madison, Wisconsin 53706, United States

Supporting Information

ABSTRACT: The highly conserved protein, IscU, serves as the scaffold for iron−sulfur cluster (ISC) assembly in the ISC system common to bacteria and eukaryotic mitochondria. The apo-form of IscU from *Escherichia coli* has been shown to populate two slowly interconverting conformational states: one structured (S) and one dynamically disordered (D). Furthermore, single-site amino acid substitutions have been shown to shift the equilibrium between the metamorphic states. Here, we report three-dimensional structural models derived from NMR spectroscopy for the S-state of wild-type (WT) apo-IscU, determined under conditions where the protein was 80% in the S-state and 20% in the D-state, and for the S-state of apo-IscU(D39A), determined under conditions where the protein was ∼95% in the S-state. We have used these structures in interpreting the effects of single site amino acid substitutions that alter %S = (100 × [S])/([S] + [D]). These include different residues at the same site, %S: D39V > D39L > D39A > D39G ≈ WT, and alanine substitutions at different sites, %S: N90A > S107A ≈ E111A > WT. Hydrophobic residues at residue 39 appear to stabilize the S-state by decreasing the flexibility of the loops that contain the conserved cysteine residues. The alanine substitutions at positions 90, 107, and 111, on the other hand, stabilize the protein without affecting the loop dynamics. In general, the stability of the S-state correlates with the compactness and thermal stability of the variant.

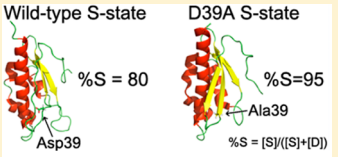

NMR Structures of Variants of *E. coli* apo-IscU

Iron-sulfur (Fe−S) clusters are ancient and ubiquitous prosthetic groups involved in a wide variety of biological processes.[1] In prokaryotes, the iron−sulfur cluster (ISC) biogenesis system, encoded by the *isc* operon (IscR, IscS, IscU, IscA, HscB, HscA, and ferredoxin), is mainly responsible for the "house-keeping" generation of iron−sulfur clusters.[2] The complex interactions of these proteins are essential for efficient Fe−S cluster biogenesis.[3] A very similar ISC system is found in the mitochondria of eukaryotes.[4] IscU is the scaffold protein for cluster assembly and transfer. The amino acid sequence of IscU is highly conserved over diverse organisms.[2] More recently, it was found that a single intronic mutation in the human *ISCU* gene is associated with a myopathy resulting from the deficiencies in Fe−S proteins succinate dehydrogenase and aconitase.[5,6] Complete removal of the *iscu* gene in mice resulted in an early embryonic death.[7]

Early NMR investigations of *Thermotoga maritima* IscU suggested that the apo-form of this protein has a "molten globule-like" structure.[8] IscU from *Haemophilus influenzae* showed a much less structured conformation in its apo-state than in its Zn^{2+}-bound state.[9] Thus, initial structural investigations of IscU focused on the Zn^{2+}-bound form of the protein.[9,10] The X-ray crystal structure of *Aquifex aeolicus* holo-IscU revealed a homotrimer with only one of the three subunits containing a [2Fe-2S] cluster. The two apo-IscU subunits adopted different conformations in the crystal.[11] It has been reported that the IscU(D39A) substitution increases the stability of the Fe−S cluster in holo-IscU.[12−14]

We found that *Escherichia coli* apo-IscU exists in solution as two interconverting conformations, one structured (S) and one dynamically disordered and lacking secondary structure (D).[15,16] The two forms interconvert on a time scale of about 1 s, and at pH 8.0 and 25 °C, the free energy difference between the two states is ∼0.5 kcal/mol.[16] A separate study from our group has demonstrated that the S ⇄ D transition involves the conversion of two peptidyl-prolyl peptide bonds from *trans* in the S-state to *cis* in the D-state (Dai, Z., Tonelli, M., and Markley, J. L., submitted for publication). Thus, although the D-state appears disordered from the lack of dispersion of its backbone NMR chemical shifts,[16] it does contain a fold that stabilizes two high-energy *cis* peptide bonds. The highly cooperative transition between the S- and D-states, which involves two concerted peptide bond isomerizations and a change in secondary structure, explains the high activation barrier and the consequent slow rates of interchange between the two states. Thus, IscU can be categorized as a metamorphic protein.[17]

Both states have been found to be physiologically important. The D-state of IscU is the substrate for IscS, the PLP-dependent cysteine desulfurase that catalyzes the conversion of cysteine to alanine and transfers the sulfane sulfur generated to IscU.[16] Once a cluster has been assembled, IscU converts to the S-state.[11] The S-state of IscU binds preferentially to HscB (the DnaJ-like cochaperone),[15] and HscB targets the complex to HscA(ATP) (the DnaK-like chaperone in its ATP-bound state). Finally, upon ATP hydrolysis HscA(ADP) binds to the

Received: May 3, 2012
Published: June 27, 2012

   dx.doi.org/10.1021/bi300579p | *Biochemistry* 2012, 51, 5557−5563

Table 1. Statistics for the Structure Determinations of the Structured States of *E. coli* apo-IscU(WT) and apo-IscU(D39A)

IscU variants [PDB]	WT [2L4X]	D39A [2KQK]
distance constraints		
intraresidue ($i = j$)	218	305
sequential ($i - j = 1$)	446	559
medium range ($1 < (i - j) \leq 5$)	416	525
long range ($i - j > 5$)	621	713
total	1701	2102
dihedral angle constraints		
φ	82	77
ψ	83	77
number of $^1D_{NH}$ RDC constraints	22	16
number of constraints per residue	14.9	17.9
number of long-range constraints per residue	4.9	5.6
CYANA target function (Å)	1.00 (±0.10)	0.98 (±0.18)
average number of distance constraints violations per conformer (>0.2 Å)	0	0
average number of dihedral angle constraints violations per conformer (°)	0	0
average r.m.s.d. for ordered residues[a] to the mean structure (Å)		
backbone atoms (N, C^α, C′)	0.5	0.4
all atoms	1.0	0.9
Ramachandran plot summary for ordered residues[a] from PROCHECK[32]		
most favored regions (%)	91.4	91.1
additionally allowed regions (%)	7.8	8.8
generously allowed regions (%)	0.8	0.1
disallowed regions (%)	0.0	0.0
PROCHECK raw score[a] (φ and ψ/all dihedral angle)	−0.50/−0.75	−0.47/−0.73
PROCHECK z-score[a] (φ and ψ/all dihedral angle)	−1.65/−4.44	−1.53/−4.32

[a]Residues 24−34, 41−58, and 72−127 of IscU(WT) and residues 26−38, 40−62, and 68−127 of IscU(D39A) were considered ordered by the Protein Structure Validation Software Suite.[28]

D-state of IscU ensuring cluster release to an acceptor protein (Kim et al., submitted for publication). IscU appears to have evolved to undergo the S ⇄ D interconversion and to have an optimal set point for this equilibrium. We found that certain single amino acid substitutions (D39A, N90A, S107A, E111A) stabilize the S-state of IscU, whereas others (K89A, N90D) stabilize the D-state.[16] In vitro Fe−S cluster assembly studies showed that IscU variants with %S = (100 × [S])/([S] + [D]) higher than wild-type (WT) assemble clusters slowly with an initial lag and that variants with %S lower than WT assemble less stable clusters at a slower rate without a lag.[16] Thus it is of considerable interest to determine the structures of the S- and D-states along with the features of the IscU sequence that are responsible for its metamorphic properties and for setting the position of the equilibrium.

We report here the solution structures of the S-states of apo-IscU(WT) and apo-IscU(D39A) determined by NMR spectroscopy. The structure of apo-IscU(WT) was determined under conditions in which %S ≈ 80; thus we had to contend with signals from the D-state of the protein. By contrast, apo-IscU(D39A) had %S ≈ 95. Comparison of structures revealed that the wild-type protein is more dynamic than the D39A variant, particularly in the cysteine-containing loops. This result suggests that the higher %S can be explained by stabilization of the S-state by the D39A substitution. The two structures have provided a framework for our analysis of data from several other single-site amino acid substitutions that alter %S.

EXPERIMENTAL PROCEDURES

Production and Purification of Proteins. We used a QuikChange II Site-Directed Mutagenesis kit (Stratagene) to mutate the pTrcIscU(WT) expression vector[18] for the production of IscU variants. Unlabeled, [U−^{15}N]- and [U−^{13}C,U−^{15}N]-labeled apo-IscU samples were produced and purified as described previously.[15,18] The elution profile of apo-IscU variants in the size exclusion chromatography using a HiLoad 16/60 Superdex 75 column (GE-Healthcare) did not show any evidence for heterogeneous oligomeric species[16] (and data not shown).

NMR Spectroscopy. The solvent used for NMR samples contained 20 mM Tris·HCl pH 8.0, 0.5 mM EDTA, 5 mM dithiothreitol, 150 mM NaCl, 7% D_2O, 0.7 mM 2,2-dimethyl-2-silapentane-5-sulfonate, and 0.02% sodium azide. A sample of 0.6−0.8 mM [U−^{15}N]-apo-IscU was employed to obtain 2D NMR spectra, while a sample of 1.5−2.0 mM [U−^{13}C,U−^{15}N]-apo-IscU was used to collect 3D NMR spectra. For measuring residual dipolar couplings (RDCs), 12−13 mg/mL Pf1 phage (Cedarlane Laboratories, Burlington, Ontario, Canada) was added to the [U−^{15}N]-apo-IscU sample.[19]

Unless specified otherwise, all NMR spectra were acquired at 25 °C with 600 or 800 MHz Varian VNMRS spectrometers equipped with a *z*-gradient cryogenic probe. We used NMRPipe[20] to process raw NMR data and SPARKY[21] for data analysis. The following data sets were collected to assign the backbone and side-chain resonances from the samples of [U−^{13}C,U−^{15}N]-apo-IscU(WT) and [U−^{13}C,U−^{15}N]-IscU(D39A): 2D ^{15}N-HSQC, 2D ^{13}C-CT-HSQC, 3D HNCO, 3D CBCA(CO)NH, 3D HNCACB, 3D C(CO)NH, 3D HBHA(CO)NH, 3D HC(CO)NH, 3D HCCH-TOCSY, 3D NOESY-^{15}N-HSQC, and 3D NOESY-^{13}C-HSQC. For assigning backbone signals of IscU(D39V), IscU(N90A), IscU(S107A), and IscU(E111A), the following data sets were collected: 2D ^{15}N-HSQC, 3D HNCO, 3D CBCA(CO)NH, and 3D HNCACB. '%S' of IscU variants were calculated from

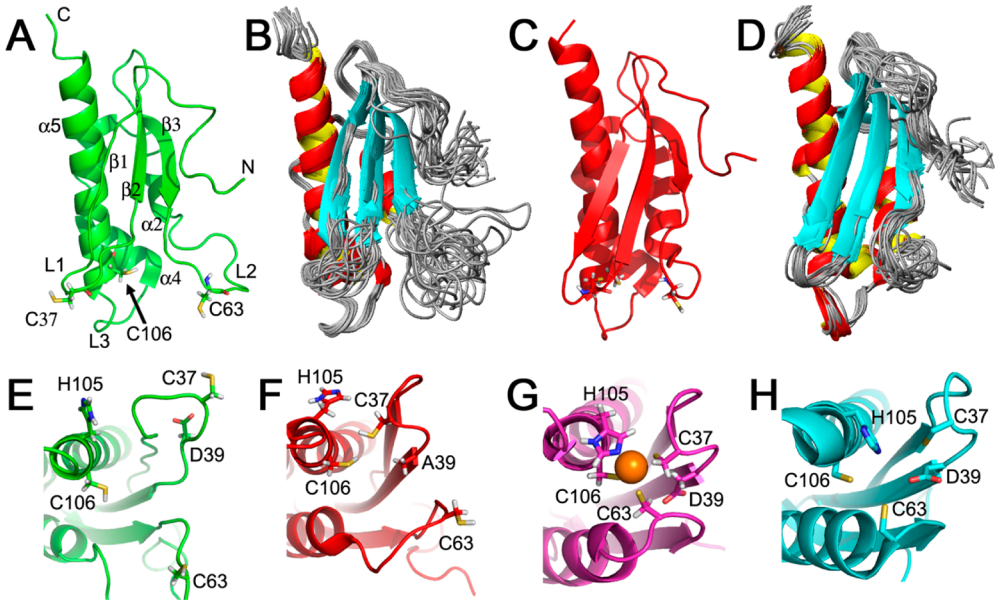

Figure 1. NMR-based models for the structured forms of apo-IscU variants. (A) Lowest energy conformer of apo-IscU(WT). (B) Overlaid 20 conformers that represent the structure of apo-IscU(WT). (C) Lowest energy conformer of apo-IscU(D39A). (D) Overlaid 20 conformers representing the structure of apo-IscU(D39A). Note that residues 1−14 are disordered and not shown in this figure. The N- and C-terminals are denoted in panel A, along with the secondary structural elements as assigned previously.[9] The loops that include highly conserved cysteine residues are also assigned as follows: the loop containing C37 is L1(35−38); the loop containing C63 is L2(60−66); the loop containing the $L^{99}PPVK^{103}$ motif[33] and flanking C106 is L3(99−103). The side chains of the three cysteine residues are shown in stick form in panels A and C. Enlargements are shown of the putative iron−sulfur cluster binding residues of (E) apo-IscU(WT) from this study; (F) apo-IscU(D39A) from this study; (G) NMR structure of Zn^{2+}-bound IscU[9] [PDB 1R9P]; and (H) X-ray structure of apo-IscU complexed with IscS[29] [PDB 3LVL] (only IscU is shown). The side chains of the residues proposed to be involved in cluster coordination[9,10] are labeled and shown in stick form. The orange sphere in panel G represents a Zn^{2+} ion.

the relative S- and D-state $^1H-^{15}N$ peak intensities from the K128 backbone or the W76 side chain by using the equation: %S = (100 × [S])/([S] + [D]). In cases where both measurements could be made, they resulted in similar %S values. $^1D_{NH}$ RDC measurements of IscU(WT) and IscU(D39A) were achieved by collecting 2D IPAP ^{15}N-HSQC spectra[22] at 25 °C on a 750 MHz Bruker DMX spectrometer equipped with a cryogenic probe.

^{15}N R_1 and R_2 relaxation rates and $^1H-^{15}N$ heteronuclear NOEs of IscU variants were measured with a 600 MHz Varian VNMRS spectrometer at 25 °C. The water flip-back scheme using water-selective pulses was employed to prevent saturation of the water resonance as well as to suppress water signals.[23] Relaxation delays of 0.1, 0.2, 0.3, 0.4, 0.6, 0.8, and 1.2 s were used to measure R_1 relaxation rates, and relaxation delays of 0.01, 0.03, 0.05, 0.07, 0.09, 0.11, and 0.13 s were used to measure R_2. For $^1H-^{15}N$ NOE experiments, ^1H excitation time was set to 3 s, and peak intensities of the 2D ^{15}N-HSQC spectra collected with and without ^1H excitation were compared to obtain $^1H-^{15}N$ NOE data. Two identical experiments were repeated to estimate standard deviations of R_1, R_2, and $^1H-^{15}N$ NOEs. The rotational correlation time (τ_c) of each IscU variant was calculated from the average R_2/R_1 value of the residues 27−33, 43−59, 73−97, and 110−125, which are not located in the flexible loops, with the following equation:[24,25] $\tau_c \approx [6(R_2/R_1)-7]^{1/2} \div (4\pi\upsilon_N)$, where υ_N is the resonance frequency of ^{15}N (60.775 MHz in our case). The relaxation rate measurements were carried out with the S-state peaks, and because the relaxation times were shorter than the lifetime of the S-state (>1.3 s), contributions from S ⇄ D exchange are expected to be small.

Structure Determination. To determine the solution structures of apo-IscU(WT) and apo-IscU(D39A), backbone and side-chain signals of IscU(D39A) were manually assigned with SPARKY.[21] The resonance assignments of IscU(D39A) were used to discriminate signals from the S-state of IscU(WT) from those of the D state. Subsequently, the peaks of 3D ^{15}N-NOESY-HSQC and 3D ^{13}C-NOESY-HSQC spectra of apo-IscU(WT) and apo-IscU(D39A) were manually picked, and CYANA 3.0[26] was used to assign them, generate distance constraints, and calculate initial structural models. TALOS+ software[27] was used to obtain backbone dihedral angle (φ and ψ) constraints. After an initial structure calculation, all assignments of the two NOESY spectra were manually inspected to repick peaks and modify assignments when necessary. $^1D_{NH}$ RDC constraints were included at the structure refinement step. The quality of the final structure was checked with the Protein Structure Validation Software Suite.[28] The statistics summarizing quality of the structure, CYANA target functions, and violations are summarized in Table 1.

Data Deposition. The 3D structural models of apo-IscU(WT) and apo-IscU(D39A) have been deposited in the Protein Data Bank (PDB ID: 2L4X and 2KQK, respectively), and the related NMR data sets have been deposited at the BioMagResBank (BMRB accession numbers 17282 and 16603, respectively). The chemical shifts and R_1, R_2, and $^1H-^{15}N$ NOE data for apo-IscU(D39V), apo-IscU(N90A), apo-IscU(S107A), and apo-IscU(E111A) have been deposited in BioMagResBank (BMRB accession numbers, 18359, 18361, 18362, 18360, respectively).

CD Spectroscopy. The buffer used for circular dichroism (CD) spectroscopy was 20 mM Tris·H_2SO_4 pH 8.0 containing 0.5 mM TCEP. We used 1-mm path length cuvettes. The

dx.doi.org/10.1021/bi300579p | *Biochemistry* 2012, 51, 5557−5563

concentration of apo-IscU was 10−20 μM. The far-UV CD spectra of IscU variants were recorded at 25 and 69 °C. Thermal denaturation curves were obtained by following CD signals at 222 nm with increasing the temperature by 3 °C steps from 9 to 69 °C. The protein samples were incubated for 5 min at each temperature. After the spectrum at 69 °C was taken, the temperature was lowered to 25 °C, and a spectrum was taken to determine the reversibility of the reaction. The reversibility was found to be on the order of 90%. Because of the variable secondary structure content of the IscU variants, the final thermal denaturation curves were normalized so that "0" represented the maximal S-state while "1" represented the minimal S-state (Figure 2S of the Supporting Information).

RESULTS

Solution Structures of the S-State Conformations of apo-IscU(WT) and apo-IscU(D39A). We overcame the difficulty posed by the heterogeneous conformation of apo-IscU[9,15] by taking advantage of the S-state stabilization of apo-IscU(D39A).[15] We first assigned the signals of apo-IscU-(D39A), whose NMR spectra were much simpler to analyze than those of apo-IscU(WT). We then assigned many of the NMR signals of apo-IscU(WT) on the basis of their similarity to those of apo-IscU(D39A). These assignments gave us starting points for extending the assignments to other signals of apo-IscU(WT) by reference to data from conventional 3D NMR experiments.

In the end, we obtained structural models for the S-states of both apo-IscU(WT) (Figure 1A,B) and apo-IscU(D39A) (Figure 1C,D). The overall fold of apo-IscU resembles those previously reported for *H. influenzae* Zn^{2+}-IscU (NMR),[9] *A. aeolicus* holo-IscU (X-ray),[11] and *E. coli* IscU in complex with IscS (X-ray).[29] Our results showed that apo-IscU has a more flexible structure than IscU in these complexes. The backbone $^{1}H-^{15}N$ cross-peaks of several residues (C37−K42, T60−S71, E98, L99, and H105) located in loops L1−L3 of apo-IscU(WT) (as denoted in Figure 1A) were not observed in 2D ^{15}N-HSQC spectra. We interpret this result to indicate that the loops adopt multiple conformations that interconvert on a millisecond time scale causing the peaks to broaden beyond detection. The flexibility of these loops is reduced somewhat in apo-IscU(D39A) (Figure 1D) as evidenced by the fewer number of unobserved backbone $^{1}H-^{15}N$ cross-peaks (A36, T60, Y61, G64−A68, and H105). The residues that have been proposed to coordinate an iron−sulfur cluster[9,10] (C37, C63, C106 and D39 or H105) are poorly packed in apo-IscU(WT) (Figure 1E), are closer together in apo-IscU(D39A) (Figure 1F), and are tightly packed in the structure of *H. influenzae* Zn^{2+}-IscU [9] (Figure 1G).

Ordering Effects of Different Amino Acids at Position 39 of IscU. Because the substitution of a charged residue with a hydrophobic residue at position 39 resulted in a more highly ordered S-state, we decided to investigate the effects of inserting amino acids of different hydrophobicity (G, A, L, V) at that site. 2D ^{15}N-HSQC spectra of these variants labeled uniformly with ^{15}N (Figure 2) showed that, whereas the %S of apo-IscU(D39G) was similar to that of apo-IscU(WT), all the hydrophobic substitutions increased %S. The effect is easily seen by comparing the intensities of the $^{1}H^{\varepsilon 1}$-$^{15}N^{\varepsilon 1}$ signals from the side chain of the single tryptophan residue (W76) in IscU (the signal on the left is from the S-state, and that on the right is from the D-state)[15,16] (boxed areas in Figure 2). We used circular dichroism (CD) spectroscopy as an independent

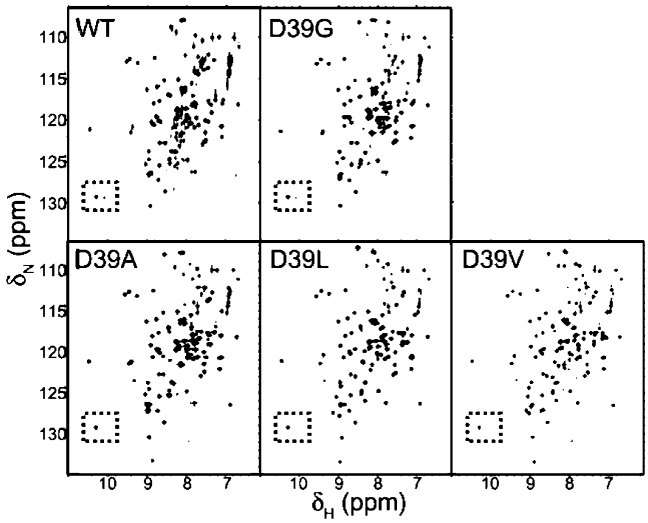

Figure 2. 2D ^{15}N-HSQC NMR spectra of [U−^{15}N]-apo-IscU variants at 25 °C, pH 8.0 and 150 mM NaCl. The relative populations of the S-state and D-state forms of these variants can be gauged from the W76 side-chain signals (boxed; left peak from the S state and right peak from the D state) and by the level of poorly dispersed peaks at the center of the spectrum from the D state. The spectra of the more structured IscU variants (D39A, D39L, and D39V) lack the D-state peak of the W76 side-chain and several poorly dispersed D-state peaks at the center of the spectrum.

measure of the conformational states of these variants. The far-UV CD spectra of the variants (Figure S1 of the Supporting Information) showed that apo-IscU(WT) and apo-IscU-(D39G) are less structured than apo-IscU(D39A), apo-IscU(D39L), or apo-IscU(D39V). We used CD spectroscopy to determine the relative thermal stabilities of S-states of the variants (Figure S2 of the Supporting Information): D39V > D39L > D39A > D39G ≈ WT.

NMR Signal Assignments of IscU Variants. To address the question of how single amino acid substitutions perturb the S ⇄ D conformational equilibrium of apo-IscU, we assigned the backbone $^{1}H-^{15}N$ NMR signals for variants with different %S values. This enabled us to determine which residues are involved in millisecond time-scale dynamics leading to disappearance of their signals (Figure 3A). For variants at position 39, we found a correlation between the number of observable cross peaks from loop residues and the %S (or thermal stability of the S-state). For example, cross peaks C37−K42, G62, C63, S69−S71, E98, and L99, which were not observed in the spectrum of WT but were found in the spectrum of D39A, were also observable in the spectrum of D39V. However, D39V exhibited additional peaks from T60 and Y61 (Figure 3A).

This correlation did not hold, however, for variants at other locations. Although apo-IscU variants N90A, S107A, and E111A exhibited %S greater than WT, their ^{15}N-HSQC spectra lacked the same $^{1}H-^{15}N$ cross peaks as WT. In some cases, these variants exhibited more dynamic loops than WT. Of the peaks observable in WT, N90A lacked the peak from L72, and E111A lacked signals from L72, V73, N90, and T91. It is clear that the S-states of these variants are stabilized by mechanisms different from those of the residue 39 variants.

The chemical shifts of several IscU variants are shown referenced to the corresponding chemical shifts of apo-IscU(WT) (Figure 3B, upper panel) and to those of apo-

dx.doi.org/10.1021/bi300579p | *Biochemistry* 2012, 51, 5557−5563

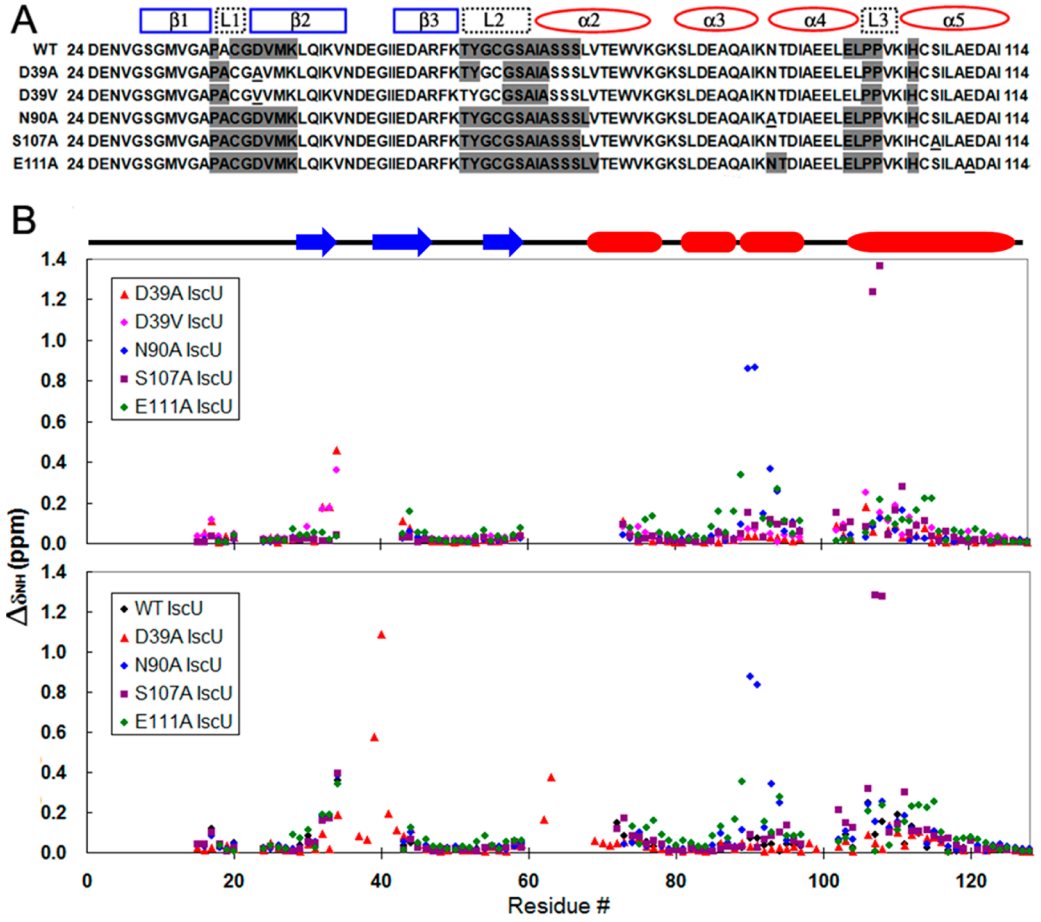

Figure 3. Analysis of assigned $^{1}H-^{15}N$ backbone signals of IscU(WT), IscU(D39A), IscU(D39V), IscU(N90A), IscU(S107A), and IscU(E111A). The secondary structural elements as observed in the structure of IscU(D39A) are marked in both panels (α-helix, red; β-strand, blue). (A) Results for residues D24–I114, the stretch showing the largest chemical shift differences between variants. Residues in this stretch whose NMR signals were not observed in 2D ^{15}N-HSQC spectra are shaded gray. The residue substituted in each IscU variant is underlined. (B) The chemical shift perturbations of IscU(WT) (black), IscU(D39A) (red), IscU(D39V) (pink), IscU(N90A) (blue), IscU(S107A) (purple), and IscU(E111A) (green) referenced to the chemical shift of IscU(WT) (upper panel) or referenced to the chemical shift of IscU(D39V), the most stable variant studied (lower panel). Aggregate ^{1}H and ^{15}N chemical shift perturbations were calculated from the equation: $\Delta\delta_{NH} = [(\Delta\delta_N/6)^2 + (\Delta\delta_H)^2]^{1/2}$.

IscU(D39V), the most thermally stable variant (Figure 3B, lower panel). As expected, the largest differences are around the sites of the substitutions. In general, the chemical shift differences in other regions are small, suggesting that the overall S-state conformations of IscU variants are similar. Still, it is noteworthy that the chemical shifts of residues located in loops L1 (C37, G38) and L2 (G62, C63), in β-strands β1 (V32–A35) and β2 (M41–Q44), and in helix α5 (C106–A110, D112–I114) deviate noticeably between IscU variants (Figure 3B). For example, substitutions at residue 39 not only affect the functionally important loops (L1–L3) but also are transmitted to more remote secondary structural elements.

Relaxation Parameters and NOEs. We measured ^{15}N R_1, R_2 values and $^{1}H-^{15}N$ heteronuclear NOEs to investigate the dynamic features of several apo-IscU variants (WT, D39A, D39V, N90A, S107A, E111A) (Figure 4). D39V and, to a lesser extent, D39A exhibited overall R_2/R_1 ratios significantly lower than WT. The R_2/R_1 ratio of a macromolecule in solution correlates with its rotational correlation time (τ_c).[24,25] From the R_2/R_1 ratios of residues not in the flexible loop regions (see Experimental Procedures for details), we determined estimates of τ_c for each apo-IscU variant: N90A, 11.4 ns; S107A, 11.1 ns; WT, 10.9 ns; E111A, 10.6 ns; D39A, 9.8 ns; D39V, 8.3 ns. Notably, the variants with the smallest molecular sizes in solution (D39A and D39V) are the ones with the most stabilized loops. By contrast, the $^{1}H-^{15}N$ NOEs of the apo-IscU variants were highly similar; this result indicates that the amino acid substitutions that alter %S (or thermal stability) do not affect dynamics on the ps–ns time scale.

DISCUSSION

We previously documented that *E. coli* apo-IscU populates two conformational states that interconvert on a subsecond time scale, one structured (S) state and one dynamically disordered (D).[15,16] We also observed that single substitutions of a few highly conserved residues (D39A, N90A, S107A, and E111A) stabilize the S-state of apo-IscU.[16] In the present study, we took advantage of the S-state stabilization of variant D39A as an aid to assigning the S-state signals of WT under conditions where the protein exists as 80% S and 20% D. The ^{1}H, ^{13}C, and ^{15}N NMR spectral assignments of these two proteins led to determination of their solution structures.

Comparison of the two structures shows that the major structural differences center on the three loops (L1–L3), which are more ordered in apo-IscU(D39A) than in apo-IscU(WT). This result prompted us to investigate a series of variants with

dx.doi.org/10.1021/bi300579p | *Biochemistry* 2012, 51, 5557–5563

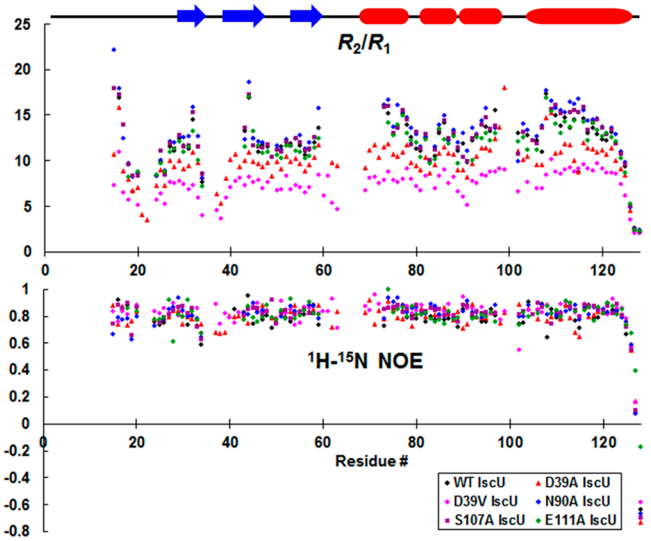

Figure 4. ^{15}N R_2/R_1 relaxation ratios (upper panel) and $^1H-^{15}N$ heteronuclear NOE values (lower panel) of IscU(WT) (black), IscU(D39A) (red), IscU(D39V) (pink), IscU(N90A) (blue), IscU-(S107A) (purple), and IscU(E111A) (green). Data were collected at 25 °C with a 600 MHz NMR spectrometer. The errors, which were estimated from the standard deviation of two replicate measurements, are not shown to simplify the figure but have been deposited along with the chemical shift data in the BioMagResBank. The secondary structural elements (α-helix, red; β-strand, blue) as determined in the structure of IscU(D39A) are marked.

residues of differing hydrophobicities at position 39. These variants exhibited differences in the dynamics of loop residues and led us to correlate the degree of rigidity of the loops with the %S (or thermal stability of the S-state) of the variant. The relative thermal stabilities of the S-states of the apo-IscU variants (D39V > D39L > D39A > D39G ≈ WT) (Figure 2S of the Supporting Information) suggest that a hydrophobic residue at this position favors the S state. The smaller rotational correlation times of D39A and D39V indicate that these apo-IscU variants are more compact than WT. Our structural model of IscU(D39A) indicates that the side chain of the substituted residue (A39) takes part in a hydrophobic cluster (Figure 1F). Apparently the hydrophobic packing energy and the entropic gain from desolvation of residues participating in the cluster overcomes the entropic loss from reduced loop flexibility. The negative charge on Asp39 appears to prevent this region from forming a stable and well-packed structure. Asp39 is a potential cluster ligand[30] and has been found to ligate the metal in the X-ray structure of a Zn^{2+}-IscU complex (PDB 2QQ4). On the other hand, H105 was found to be the cluster ligand in the NMR structures of another Zn^{2+}-IscU complex[9] and in the X-ray structure of [2Fe-2S]-IscU(D39A).[11] If H105 is the fourth ligand, the negative charge on D39 will be countered by the positive charge on the assembled cluster.

The L1−L3 loops of IscU are well-packed in the NMR structure of the Zn^{2+}-IscU complex[9] (Figure 1G) and in the X-ray crystal structure of apo-IscU complexed with IscS[29] (Figure 1H). We have shown by NMR spectroscopy that the D-state of apo-IscU binds to and is stabilized by the cysteine desulfurase (IscS).[16] In the X-ray structure of apo-IscU:IscS,[29] crystal packing forces appear to have trapped apo-IscU in the S-state, which in solution becomes populated only during or after Fe−S cluster formation. The recent X-ray structure of the [2Fe-2S]-IscS-IscU(D35A) complex from *Archaeoglobus fulgidus*[30] demonstrated that IscU is in the S-state in this complex. The two conformational states of apo-IscU (S and D) are selected by different proteins involved in Fe−S cluster assembly and delivery, and their existence appears not to be an artifact resulting from the absence of a cofactor or partner protein as has been proposed.[31]

Our results show that the flexibility of the L1−L3 loops of the S-state of apo-IscU(WT) is dictated by the protein sequence. The highly conserved and solvent-exposed hydrophobic residues Met31 and Val40, which have been shown to interact with HscB,[15] are better packed in IscU(D39A) than in the wild-type protein. HscB interacts preferentially with the S-state of apo-IscU,[15] and its physiological role is to bind to holo-IscU, which is stabilized in the S-state. It appears that the interaction between HscB and IscU is stronger when the region containing Met31, Asp39, and Val40 is stably packed.

Our studies of apo-IscU variants (N90A, S107A, E111A) show that the S-state can be stabilized by mechanisms that do not involve the loops. Differences between the chemical shifts of these apo-IscU variants and WT suggest that interactions between helices α3-α4 and helix α5 may be responsible for stabilizing the S-state. Because D39A and D39V also showed perturbed chemical shifts in these regions, L1−L3 loop stabilization may be transmitted to the helices as part of the mechanism for increasing %S.

■ ASSOCIATED CONTENT

Supporting Information

Far-UV CD spectra of apo-IscU variants (Figure S1), and their thermal stabilities measured with CD spectroscopy (Figure S2). This material is available free of charge via the Internet at http://pubs.acs.org.

■ AUTHOR INFORMATION

Corresponding Author

*Telephone: (608) 263-9349; e-mail: markley@nmrfam.wisc.edu.

Funding

This work was supported by U.S. National Institutes of Health (NIH) Grants R01 GM58667 and U01 GM94622 and was a collaboration with the National Magnetic Resonance Facility at Madison which is supported by NIH grants from the National Center for Research Resources (5P41RR002301-27) and the National Institute of General Medical Sciences (8 P41 GM103399-27).

Notes

The authors declare no competing financial interest.

■ ABBREVIATIONS USED:

EDTA, 2,2′,2″,2‴-(ethane-1,2-diyldinitrilo)tetraacetic acid; HSQC, heteronuclear single-quantum correlation; NMR, nuclear magnetic resonance; NOE, nuclear Overhauser enhancement; TCEP, 3,3′,3″-phosphanetriyltripropanoic acid; PLP, pyridoxal-5′-phosphate; WT, wild type

■ REFERENCES

(1) Beinert, H., Holm, R. H., and Munck, E. (1997) Iron-sulfur clusters: Nature's modular, multipurpose structures. *Science 277*, 653−659.

(2) Zheng, L., Cash, V. L., Flint, D. H., and Dean, D. R. (1998) Assembly of iron-sulfur clusters. Identification of an iscSUA-hscBA-fdx

gene cluster from *Azotobacter vinelandii*. *J. Biol. Chem. 273*, 13264−13272.
(3) Johnson, D. C., Dean, D. R., Smith, A. D., and Johnson, M. K. (2005) Structure, function, and formation of biological iron-sulfur clusters. *Annu. Rev. Biochem. 74*, 247−281.
(4) Lill, R. (2009) Function and biogenesis of iron-sulphur proteins. *Nature 460*, 831−838.
(5) Mochel, F., Knight, M. A., Tong, W. H., Hernandez, D., Ayyad, K., Taivassalo, T., Andersen, P. M., Singleton, A., Rouault, T. A., Fischbeck, K. H., and Haller, R. G. (2008) Splice mutation in the iron-sulfur cluster scaffold protein ISCU causes myopathy with exercise intolerance. *Am. J. Hum. Genet. 82*, 652−660.
(6) Olsson, A., Lind, L., Thornell, L. E., and Holmberg, M. (2008) Myopathy with lactic acidosis is linked to chromosome 12q23.3−24.11 and caused by an intron mutation in the ISCU gene resulting in a splicing defect. *Hum. Mol. Genet. 17*, 1666−1672.
(7) Nordin, A., Larsson, E., Thornell, L. E., and Holmberg, M. (2011) Tissue-specific splicing of ISCU results in a skeletal muscle phenotype in myopathy with lactic acidosis, while complete loss of ISCU results in early embryonic death in mice. *Hum. Genet. 129*, 371−378.
(8) Bertini, I., Cowan, J. A., Del Bianco, C., Luchinat, C., and Mansy, S. S. (2003) *Thermotoga maritima* IscU. Structural characterization and dynamics of a new class of metallochaperone. *J. Mol. Biol. 331*, 907−924.
(9) Ramelot, T. A., Cort, J. R., Goldsmith-Fischman, S., Kornhaber, G. J., Xiao, R., Shastry, R., Acton, T. B., Honig, B., Montelione, G. T., and Kennedy, M. A. (2004) Solution NMR structure of the iron-sulfur cluster assembly protein U (IscU) with zinc bound at the active site. *J. Mol. Biol. 344*, 567−583.
(10) Liu, J., Oganesyan, N., Shin, D. H., Jancarik, J., Yokota, H., Kim, R., and Kim, S. H. (2005) Structural characterization of an iron-sulfur cluster assembly protein IscU in a zinc-bound form. *Proteins 59*, 875−881.
(11) Shimomura, Y., Wada, K., Fukuyama, K., and Takahashi, Y. (2008) The asymmetric trimeric architecture of [2Fe-2S] IscU: implications for its scaffolding during iron-sulfur cluster biosynthesis. *J. Mol. Biol. 383*, 133−143.
(12) Unciuleac, M. C., Chandramouli, K., Naik, S., Mayer, S., Huynh, B. H., Johnson, M. K., and Dean, D. R. (2007) In vitro activation of apo-aconitase using a [4Fe-4S] cluster-loaded form of the IscU [Fe-S] cluster scaffolding protein. *Biochemistry 46*, 6812−6821.
(13) Wu, G., Mansy, S. S., Wu, Sp, S. P., Surerus, K. K., Foster, M. W., and Cowan, J. A. (2002) Characterization of an iron-sulfur cluster assembly protein (ISU1) from *Schizosaccharomyces pombe*. *Biochemistry 41*, 5024−5032.
(14) Foster, M. W., Mansy, S. S., Hwang, J., Penner-Hahn, J. E., Surerus, K. K., and Cowan, J. A. (2000) A mutant human IscU protein contains a stable [2Fe-2S](2+) center of possible functional significance. *J. Am. Chem. Soc. 122*, 6805−6806.
(15) Kim, J. H., Füzéry, A. K., Tonelli, M., Ta, D. T., Westler, W. M., Vickery, L. E., and Markley, J. L. (2009) Structure and dynamics of the iron-sulfur cluster assembly scaffold protein IscU and its interaction with the cochaperone HscB. *Biochemistry 48*, 6062−6071.
(16) Kim, J. H., Tonelli, M., and Markley, J. L. (2012) Disordered form of the scaffold protein IscU is the substrate for iron-sulfur cluster assembly on cysteine desulfurase. *Proc. Natl. Acad. Sci. U.S.A. 109*, 454−459.
(17) Murzin, A. G. (2008) Biochemistry - Metamorphic proteins. *Science 320*, 1725−1726.
(18) Hoff, K. G., Silberg, J. J., and Vickery, L. E. (2000) Interaction of the iron-sulfur cluster assembly protein IscU with the Hsc66/Hsc20 molecular chaperone system of *Escherichia coli*. *Proc. Natl. Acad. Sci. U.S.A. 97*, 7790−7795.
(19) Hansen, M. R., Mueller, L., and Pardi, A. (1998) Tunable alignment of macromolecules by filamentous phage yields dipolar coupling interactions. *Nat. Struct. Biol. 5*, 1065−1074.
(20) Delaglio, F., Grzesiek, S., Vuister, G. W., Zhu, G., Pfeifer, J., and Bax, A. (1995) NMRPIPE - A multidimensional spectral processing system based on UNIX pipes. *J. Biomol. NMR 6*, 277−293.
(21) Goddard, T. D., Kneller, D. G. (2008) Sparky 3, University of California, San Francisco, San Francisco.
(22) Ottiger, M., Delaglio, F., and Bax, A. (1998) Measurement of J and dipolar couplings from simplified two-dimensional NMR spectra. *J. Magn. Reson. 131*, 373−378.
(23) Grzesiek, S., and Bax, A. (1993) The importance of not saturating H_2O in protein NMR. Application to sensitivity enhancement and NOE measurements. *J. Am. Chem. Soc. 115*, 12593−12594.
(24) Aramini, J. M., Tubbs, J. L., Kanugula, S., Rossi, P., Ertekin, A., Maglaqui, M., Hamilton, K., Ciccosanti, C. T., Jiang, M., Xiao, R., Soong, T. T., Rost, B., Acton, T. B., Everett, J. K., Pegg, A. E., Tainer, J. A., and Montelione, G. T. (2010) Structural basis of O6-alkylguanine recognition by a bacterial alkyltransferase-like DNA repair protein. *J. Biol. Chem. 285*, 13736−13741.
(25) Kay, L. E., Torchia, D. A., and Bax, A. (1989) Backbone dynamics of proteins as studied by ^{15}N inverse detected heteronuclear NMR spectroscopy: Application to staphylococcal nuclease. *Biochemistry 28*, 8972−8979.
(26) Güntert, P. (2004) Automated NMR structure calculation with CYANA. *Methods Mol. Biol. 278*, 353−378.
(27) Shen, Y., Delaglio, F., Cornilescu, G., and Bax, A. (2009) TALOS+: a hybrid method for predicting protein backbone torsion angles from NMR chemical shifts. *J. Biomol. NMR 44*, 213−223.
(28) Bhattacharya, A., Tejero, R., and Montelione, G. T. (2007) Evaluating protein structures determined by structural genomics consortia. *Proteins 66*, 778−795.
(29) Shi, R., Proteau, A., Villarroya, M., Moukadiri, I., Zhang, L., Trempe, J. F., Matte, A., Armengod, M. E., and Cygler, M. (2010) Structural basis for Fe-S cluster assembly and tRNA thiolation mediated by IscS protein-protein interactions. *PLoS Biol. 8*, e1000354.
(30) Marinoni, E. N., de Oliveira, J. S., Nicolet, Y., Raulfs, E. C., Amara, P., Dean, D. R., and Fontecilla-Camps, J. C. (2012) $(IscS\text{-}IscU)_2$ Complex Structures Provide Insights into Fe_2S_2 Biogenesis and Transfer. *Angew. Chem., Int. Ed. 51*, 1−5.
(31) Prischi, F., Pastore, C., Carroni, M., Iannuzzi, C., Adinolfi, S., Temussi, P., and Pastore, A. (2010) Of the vulnerability of orphan complex proteins: the case study of the *E. coli* IscU and IscS proteins. *Protein Expr. Purif. 73*, 161−166.
(32) Laskowski, R. A., MacArthur, M. W., Moss, D. S., and Thornton, J. M. (1993) PROCHECK - a program to check the stereochemical quality of protein structures. *J. App. Cryst. 26*, 283−291.
(33) Hoff, K. G., Cupp-Vickery, J. R., and Vickery, L. E. (2003) Contributions of the LPPVK motif of the iron-sulfur template protein IscU to interactions with the Hsc66-Hsc20 chaperone system. *J. Biol. Chem. 278*, 37582−37589.